*35th EPS Conference on Plasma Phys. Hersonissos, 9 - 13 June 2008 ECA Vol.**32D**, P-2.021 (2008)*

Bicoherence and Confinement Transitions at TJ-II

B.Ph. van Milligen, T. Kalhoff, M.A. Pedrosa, C. Hidalgo

Asociación EURATOM-CIEMAT para Fusión,

Avda. Complutense 22, 28040 Madrid, Spain

In the flexible heliac TJ-II, confinement transitions are observed, either induced (by applying biasing) or spontaneous. The improved confinement state is mainly characterised by a higher (energy and particle) confinement time, which is reflected in, e.g., a higher value of the electron density, and correspondingly higher values of the density gradient near the edge. The confinement transition is associated with the formation of a shear flow layer in the edge [1].

Indeed, sheared flow is an important theoretical ingredient of models attempting to explain such confinement transitions [2]. The generation of sheared flow should be accompanied by a detectable increase of bicoherence [3,4]. The stellarator TJ-II is in a unique position to investigate this issue due to the specific magnetic configuration of this device: the transitions at TJ-II are 'soft' and the plasma can remain close to the transition for some time and cross the critical point 'slowly', thus allowing a study of the evolution of parameters during the transition.

The outline of this paper is as follows: first, we discuss the experimental set-up and methods used, and then we present the results from biasing experiments and spontaneous transitions.

Experimental set-up and methods

Here, we study discharges with either forced or spontaneous confinement transitions at the flexible heliac TJ-II [5]. The plasmas studied have a toroidal magnetic field of $B_T = 1$ T, major radius $R = 1.5$ m, mean minor radius $\langle a \rangle = 0.22$ m, and rotational transform $\iota(a) \sim 1.6 \acute{} 1.8$. The plasmas are heated using Electron Cyclotron Resonant Heating with power $P_{ECRH} = 200 \acute{} 400$ kW. The discharges studies here have been analysed earlier from a different perspective [1,6]. Data are taken with a reciprocating multiple Langmuir probe system [7], sampling at 2 MHz. Signals studied include the ion saturation current I_{sat}, the floating potential V_f, and the poloidal electric field calculated as $E_\theta \propto V_f^1 - V_f^2$. The Fourier-based bicoherence analysis applied is standard [8].

Biasing experiments

In these experiments, a biasing electrode was inserted about 2 cm into the plasma and biased with respect to a poloidal limiter, tangent to the Last Closed Flux Surface (LCFS) [1]. On a shot by shot basis, the radial probe position $\rho = r/a$ was varied. Biasing was applied in the time window $1100 < t < 1150$ (when $\rho < 0.99$) or $1100 < t < 1170$ (when $\rho \geq 0.99$). Fig. 1 shows the Root Mean Square (RMS) variation of E_θ vs. time and position, normalised to the mean RMS of the same data over the whole time window shown. The reduction of the fluctuation level during the biasing time interval is evident across all radii. After biasing is switched off, the fluctuation level is high because the density has increased during the biasing time interval (and therefore the associated fluctuation level). Afterwards, the fluctuation level decays as the density decays.

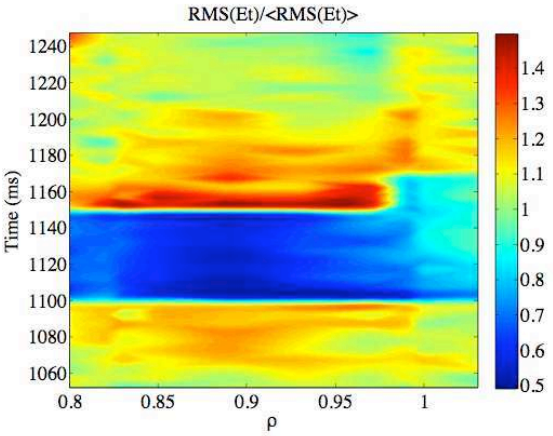

Fig. 1: Fluctuation level response to biasing; RMS(E_θ) /⟨ RMS(E_θ)⟩

Fig. 2 shows a typical result for the auto-bicoherence of E_θ at a radial position (ρ = 0.97) and in a time interval where the bicoherence is high. Fig. 3 shows the summed auto-bicoherence for the same data selection, along with the summed auto-bicoherence computed in a later time window (after biasing), and the corresponding statistical error level. This plot shows that the auto-bicoherence is statistically significant at this radial position during biasing, at least for relatively low frequencies.

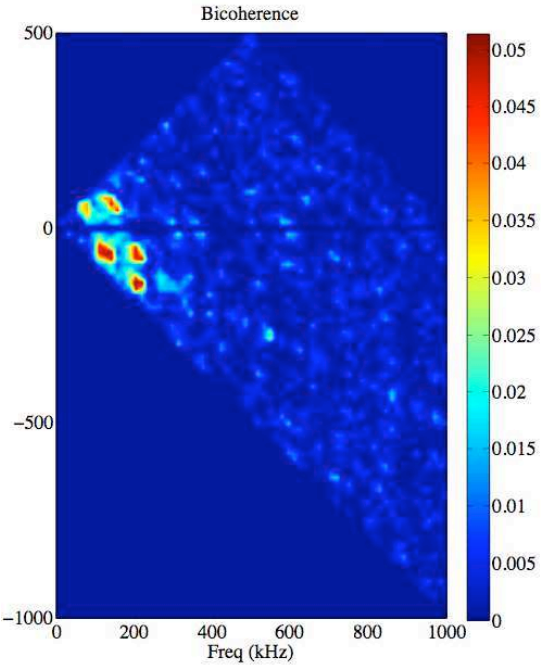

Fig. 2: Typical auto-bicoherence graph (E_θ). High values occur for $f < 250$ kHz

Since the significant bicoherence is concentrated in the low frequency range, we will calculate the total bicoherence (the area integral of Fig. 2) by integrating only over the low frequencies (f_1, f_2, $f_1+f_2 \leq 250$ kHz). Evaluating the total auto-bicoherence of E_θ in this manner for all available times and radii, we obtain Fig. 4. The response of the bicoherence to the biasing, applied in the time intervals

given above, is clearly visible in the radial range $0.9 < \rho < 1$. Recall that the biasing electrode was inserted about 2 cm into the plasma, corresponding to a position of $\rho \approx 0.9$. High values of the bicoherence occurring outside the plasma ($\rho > 1$) are deemed not to be significant. This plot suggests that the applied external biasing induces three-wave coupling in a narrow radial range, coinciding with the flow shear layer. Comparing this figure with Fig. 1, it is evident that the detected bicoherence is not just caused by a reduction of turbulence amplitude, since that reduction occurs across all radii whereas the bicoherence is localised. Conversely, it is evident that the turbulence is suppressed in a far wider radial range than the range where the bicoherence is concentrated.

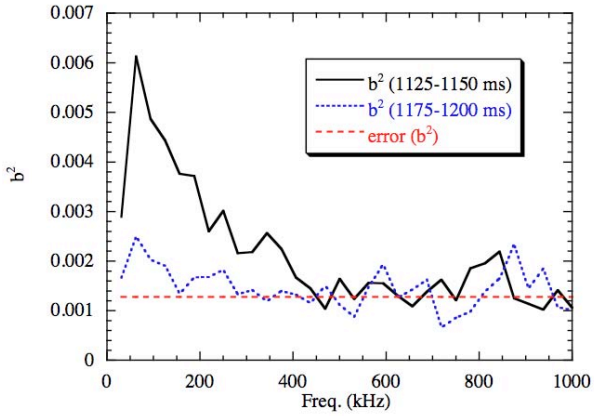

Fig. 3: Summed auto-bicoherence (E_θ) during and after biasing

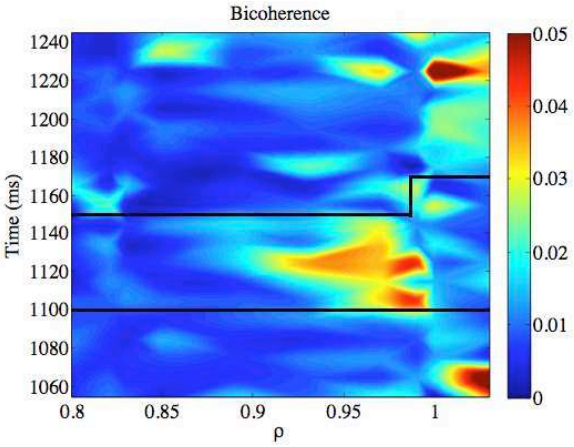

Fig. 4: Total low-frequency auto-bicoherence (E_θ) vs. ρ and t. Lines indicate biasing.

Spontaneous transitions

Spontaneous confinement transitions are routinely observed at TJ-II. As the line average density increases, a velocity shear layer is generated at the edge of the plasma. Although the ´true' parameter underlying the transition is not known, in practice the line average density acts as its proxy in TJ-II, in the sense that the transition often occurs at the same or similar values of the density. When the critical value of this parameter is exceeded, turbulence levels decrease and (energy and particle) confinement improves.

We have analysed a set of discharges with slowly evolving line average density and spontaneous confinement transitions [1,6]. In these discharges, the density rises and then decays, producing two passages through the critical point. From a set of six such discharges, only one showed a clear response in the bicoherence, namely the one where the Langmuir probe was located at $\rho = 0.87$. The fact that this radial position is different than the position of maximum bicoherence in the biasing cases (previous section) may either be ascribed to the different discharge conditions (e.g., the density is much higher here), or to the fact that the

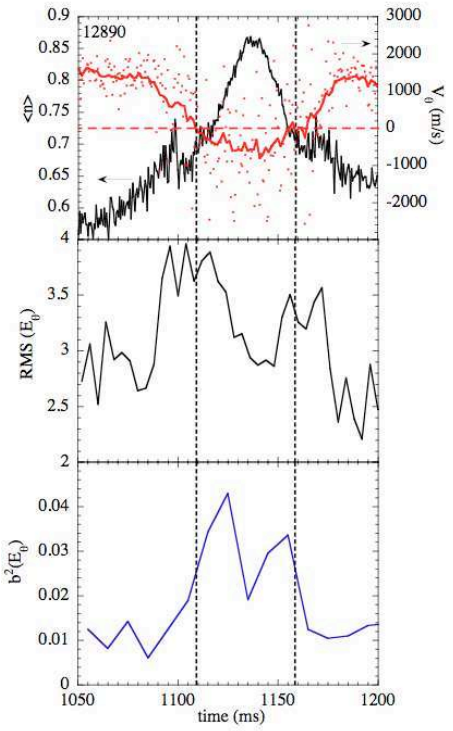

Fig. 5: Spontaneous transition. Top: line density (10^{19} m^{-3}) and poloidal phase velocity; Centre: RMS(E_θ); Bottom: auto-bicoherence (E_θ)

location of the biasing electrode dictates the shear layer position in the biasing experiments. Fig. 5 shows the evolution of the line average density and the poloidal phase velocity (calculated from the floating potential measured at poloidally separated probe pins). The vertical dashed lines mark the zero crossings of the phase velocity. The time interval between these two vertical lines is the improved confinement region, as evidenced by a drop in fluctuation level (visible in the density time trace) and a sharp increase of the line density. The central plot shows RMS(E_θ). The confinement transitions (marked by the vertical dashed lines) are characterised by an increased RMS level, as expected for phase transitions. In the improved state (between the dashed lines), the RMS level drops. Here, it does not drop to values below the low confinement state, because the plasma makes a back-transition before this can happen. In the time interval corresponding to the improved state, the bicoherence reaches a level that is 3 to 4 times above the level outside this time interval. The rising and falling flanks of the bicoherence traces correspond to the maxima of RMS(E_θ) ´ i.e., shear flow growth and decay near the confinement transitions ´, while the highest bicoherence values occur during the improved state near the transitions, in qualitative agreement with theoretical expectations from shear flow models.

References

[1] M. Pedrosa, C. Hidalgo, *et al.*, Plasma Phys. Control. Fusion **47**, 777 (2005)

[2] C. Hidalgo, B. van Milligen, M. Pedrosa, Comptes Rendus Physique **7**, 679 (2006)

[3] P. Diamond, M. Rosenbluth, *et al.*, Phys. Rev. Lett. **84**, 4842 (2000)

[4] K. Itoh, Y. Nagashima, *et al.*, Phys.Plasmas **12**, 102301 (2005)

[5] C. Alejaldre, J. Alonso, *et al.*, Plasma Phys. Control. Fusion **41**, A539 (1999)

[6] B. Carreras, L. García, M. Pedrosa, and C. Hidalgo, Phys. Plasmas **13**, 122509 (2006)

[7] M. Pedrosa, A. López-Sánchez, C. Hidalgo, *et al.*, Rev. Sci. Instrum. **70**, 415 (1999)

[8] B. van Milligen, E. Sánchez, *et al.*, Phys. Plasmas **2**, 3017 (1995)